Late Quaternary lake-level changes constrained by radiocarbon and stable isotope studies on sediment cores from Lake Titicaca, South America

Harold D. Rowe
Geological and Environmental Sciences, Stanford University, Bldg. 320, Rm. 118, Stanford, CA

Thomas P. Guilderson
Center for Accelerator Mass Spectrometry, Lawrence Livermore National Laboratory, Livermore, CA

Robert B. Dunbar
Geological and Environmental Sciences, Stanford University, Bldg. 320, Rm. 118, Stanford, CA

John R. Southon
Center for Accelerator Mass Spectrometry, Lawrence Livermore National Laboratory, Livermore, CA

Geoffrey O. Seltzer
Syracuse University

See next page for additional authors

Authors
Harold D. Rowe, Thomas P. Guilderson, Robert B. Dunbar, John R. Southon, Geoffrey O. Seltzer, David A. Mucciarone, Sherilyn C. Fritz, and Paul A. Baker

Available online at www.sciencedirect.com
SCIENCE DIRECT
ELSEVIER
Global and Planetary Change 38 (2003) 273–290
GLOBAL AND PLANETARY CHANGE
www.elsevier.com/locate/gloplacha

Late Quaternary lake-level changes constrained by radiocarbon and stable isotope studies on sediment cores from Lake Titicaca, South America

Harold D. Rowe[a,b,*], Thomas P. Guilderson[c,d], Robert B. Dunbar[a], John R. Southon[c], Geoffrey O. Seltzer[e], David A. Mucciarone[a], Sherilyn C. Fritz[f], Paul A. Baker[g]

[a] *Geological and Environmental Sciences, Stanford University, Bldg. 320, Rm. 118, Stanford, CA 94305-2115, USA*
[b] *Earth and Environmental Sciences, University of Illinois at Chicago, SES Bldg., MC-186, 845 West Taylor Avenue, Chicago, IL 60607-7059, USA*
[c] *Center for Accelerator Mass Spectrometry, Lawrence Livermore National Laboratory, Livermore, CA 94551, USA*
[d] *Department of Ocean Sciences and Institute of Marine Sciences, Earth and Marine Sciences Bldg., Rm. A316, University of California, Santa Cruz, Santa Cruz, CA 95064, USA*
[e] *Department of Earth Sciences, 204 Heroy Geology Laboratory, Syracuse University, Syracuse, NY 13244-1070, USA*
[f] *Department of Geosciences, 214 Bessey Hall, University of Nebraska-Lincoln, Lincoln, NE 68588-0340, USA*
[g] *Division of Earth and Ocean Sciences, Duke University, Box 90227, Durham, NC 27708-0227, USA*

Received 25 November 2001; accepted 9 April 2002

Abstract

We present and compare AMS-^{14}C geochronologies for sediment cores recovered from Lake Titicaca, South America. Radiocarbon dates from three core sites constrain the timing of late Quaternary paleoenvironmental changes in the Central Andes and highlight the site-specific factors that limit the radiocarbon geochronometer. With the exception of mid-Holocene sediments, all cores are generally devoid of macrophyte fragments, thus bulk organic fractions are used to build core chronologies. Comparisons of radiocarbon results for chemically defined fractions (bulk decalcified, humate, humin) suggest that ages derived from all fractions are generally coherent in the post-13,500 yr BP time interval. In the pre-13,500 yr BP time interval, ages derived from humate extracts are significantly younger (300–7000 years) than ages from paired humin residues. Gross age incoherencies between paired humate and humin sub-fractions in pre-13,500 yr BP sediments from all core sites probably reflect the net downward migration of humates. Ages derived from bulk decalcified fractions at our shallow water (90 m) and deep water (230 m) core sites consistently fall between ages derived from humate and humin sub-fractions in the pre-13,500 yr BP interval, reflecting that the bulk decalcified fraction is predominantly a mixture of humate and humin sub-fractions. Bulk decalcified ages from the pre-13,500 yr BP interval at our intermediate depth core site (150 m) are consistently older than humate (youngest) and humin sub-fractions. This uniform, reproducible pattern can

* Corresponding author. Department of Geological Sciences, University of Kentucky, 101 Slone Research Bldg., Lexington, KY 40506-0053, USA. Tel.: +1-859-257-2770; fax: +859-257-2770.

E-mail addresses: hrowe@uky.edu (H.D. Rowe), guilderson1@llnl.gov (T.P. Guilderson), dunbar@pangea.stanford.edu (R.B. Dunbar), southon1@llnl.gov (J.R. Southon), goseltze@mailbox.syr.edu (G.O. Seltzer), dam@pangea.stanford.edu (D.A. Mucciarone), sfritz2@unl.edu (S.C. Fritz), pbaker@geo.duke.edu (P.A. Baker).

0921-8181/$ - see front matter
doi:10.1016/S0921-8181(03)00031-6

be explained by the mobilization of a relatively older organic sub-fraction during and after the re-acidification step following the alkaline treatment of the bulk sediment. The inferred existence of this 'alkali-mobile, acid-soluble' sub-fraction implies a different depositional/post-depositional history that is potentially associated with a difference in source material. While internally consistent geochronologies can be developed for the Lake Titicaca sequence using different organic fractions, mobile organic sub-fractions and fractions containing mobile sub-fractions should generally be avoided in geochronology studies. Consequently, we believe humin and/or bulk decalcified ages provide the most consistent chronologies for the post-13,500 yr BP interval, and humin ages provide the most representative ages for sedimentation prior to 13,500 yr BP interval.

Using the age model derived from the deep water core site and a previously published isotope-based lake-level reconstruction, we present a qualitative record of lake level in the context of several ice-core records from the western hemisphere. We find the latest Pleistocene lake-level response to changing insolation began during or just prior to the Bølling/Allerød period. Using the isotope-based lake-level reconstruction, we also find the 85-m drop in lake level that occurred during the mid-Holocene was synchronous with an increase in the variability of ice-core $\delta^{18}O$ from a nearby icecap, but was not reflected in any of the polar ice-core records recovered from the interior of Antarctica and Greenland.

Keywords: Paleoclimate; Radiocarbon; Lake sediments; Humin; Humate; South America

1. Introduction

Accurate age models are vitally important for the identification of leads and lags in paleoclimate records (Pilcher, 1991; Lowe and Walker, 2000). Although studies of late Quaternary lacustrine facies rely almost exclusively on the AMS-^{14}C method for age control, most studies do not incorporate the large number of radiocarbon measurements that are necessary to address changing reservoir-water effects and constrain the timing of changes in sedimentation rates (Lowe, 1991, and references therein; Hammarlund et al., 1997). Attempts to quantify and correct for uncertainties must compare the age results of chemically and/or physically separable fractions (macrophytes, pollen, bulk organic matter, humate, and humin) from discrete intervals (Shore et al., 1995; Abbott and Stafford, 1996; Van Klinken and Hedges, 1998). Barring reservoir-water effects (those effects that occur when materials have incorporated carbon from aqueous bicarbonate derived from an old source; Shotton, 1972), age coherency between isolated fractions from a discrete interval can be taken as evidence for acceptance of an age of sedimentation. Age incoherency between fractions demands a plausible explanation for the discrepancy and elimination of the "contaminating" fraction(s).

Sites with sound geochronologies and calibrated proxy records provide the most useful paleoclimate/paleoecological information. Reconstructions of past environmental conditions from low-latitude sites provide important clues for identifying the forcing mechanisms responsible for climate change at millennial and submillennial timescales (e.g., Guilderson et al., 1994, 2001; deMenocal et al., 2000a). We present down-core AMS-^{14}C ages for chemically defined organic fractions from Lake Titicaca (16°S, 69°W; 3810 m asl), South America. Lake level has fluctuated by tens of meters during the last glacial/interglacial cycle, reaching a lowstand of 85 m below modern level during the middle Holocene (Wirrmann and de Oliveira Almeida, 1987; Mourguiart, 1990; Wirrmann et al., 1990, 1992; Wirrmann and Mourguiart, 1995; Abbott et al., 1997a,b; Mourguiart et al., 1998; Seltzer et al., 1997; Cross et al., 1999; Baker et al., 2001; Rowe et al., 2002). Although two lake-level proxy indicators (bulk organic $\delta^{13}C$, diatoms) are now recognized (Baker et al., 2001; Rowe et al., 2002), a detailed geochronology for the late Quaternary has not yet been established. This paper focuses on the radiocarbon geochronology, addressing the specific challenges of using ^{14}C as a dating tool at Lake Titicaca, and presenting the isotope-based paleoenvironmental record in the context of a new age model.

The Titicaca drainage basin (57,340 km^2) occupies the northern third of the high-altitude tectonic plateau known as the South American Altiplano (Fig. 1a). Regional moisture originates from the tropical Atlantic

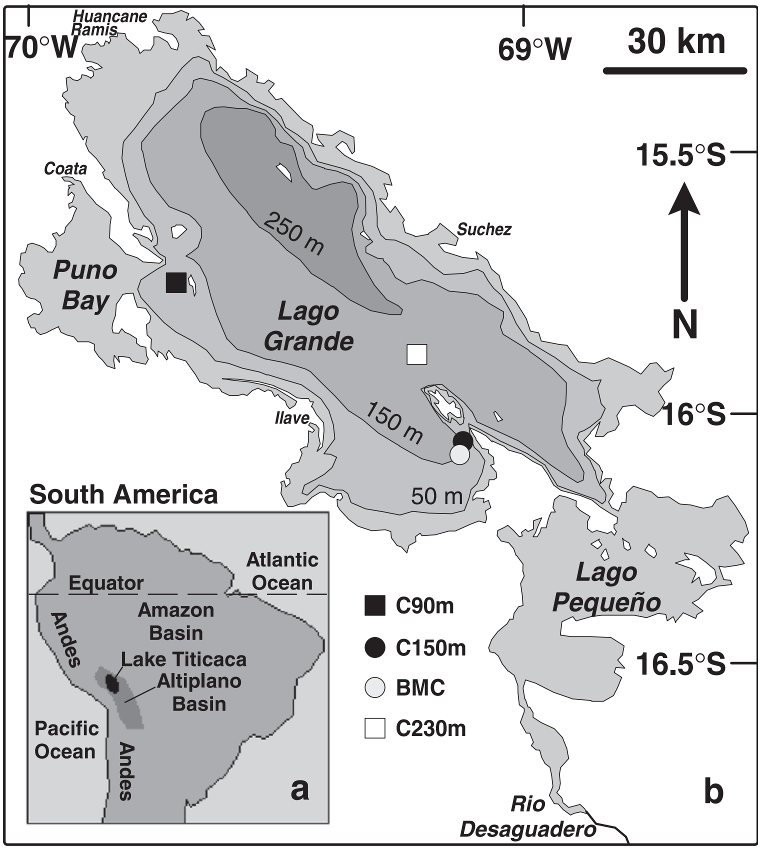

Fig. 1. (a) The location of Lake Titicaca with respect to the South American Altiplano and the Amazon Basin. (b) Map of Lake Titicaca showing core site and geographical locations. Italicized proper names illustrate inflow location of major rivers.

Ocean and is transported to the Altiplano during the austral summer (DJF) by the coupled interaction of deep convection in the Amazon Basin and middle- and upper-level easterlies associated with the Bolivian High, an interaction establishing what is now termed the South American Summer Monsoon (SASM; Zhou and Lau, 1998; Garreaud, 1999, 2000; Lenters and Cook, 1999; Vuille, 1999). Most rivers on the northern Altiplano drain into Lake Titicaca (area = 8562 km^2, volume = 903.7 × 10^9 m^3, Wirrmann, 1992), and the lake drains to the south by way of the Rio Desaguadero. Direct evaporation accounts for ~ 95% of the annual water loss (Monnheim, 1956). Historical lake-level changes of ± 3 m largely reflect interannual variability of moisture transport to the northern Altiplano (Roche et al., 1992). Recent studies of the modern climate

Table 1
Location, water depth, and core length for the core sites used in this study

Core site	Core	Latitude (°S)	Longitude (°W)	Water depth (m)	Core length (m)
C90m	NE97-7PC	15°48.381′	69°42.096′	89	8.330
	NE98-10BXA	15°48.392′	69°42.117′	90	0.970
C150m	NE98-1PC	16°08.004′	69°09.199′	152	10.600
	NE98-4BXB	16°08.259′	69°09.267′	147	0.845
	BMC	16°08.004′	69°09.199′	152	8.100
C230m	NE97-2PC	15°52.441′	69°17.462′	230	7.865

Table 2
Raw and calibrated radiocarbon results for all fractions and the corresponding sediment depths for core site C90m

Laboratory accession no.	Depth below sediment surface (cm)	Fraction dated	^{14}C age	Error	+ 1s yr BP	Rounded yr BP INTCAL98	− 1s yr BP	Coral calibrated age yr BP	Model age yr BP
OS-19791	5.0	BD	180	45	100	50	10	–	50*
OS-20624	50.0	BD	1020	30	710	680	670	–	680*
OS-19792	95.0	BD	1610	70	1310	1290	1190	–	1290*
OS-17702	176.5	BD	2630	25	2360	2350	2350	–	2350*
CAMS-70682	209.5	BD	3350	40	3360	3280	3270	–	3280*
CAMS-70683	238.5	BD	3680	40	3720	3660	3640	–	3660*
CAMS-70684	268.5	BD	4170	40	4420	4410	4300	–	4410*
CAMS-70685	288.5	BD	4380	40	4810	4620	4530	–	4620*
CAMS-70686	313.5	BD	4720	40	5280	5190	4980	–	5190*
CAMS-70687	338.5	BD	4850	40	5440	5310	5300	–	5310*
OS-20113	363.5	BD	5300	50	5890	5830	5730	–	5830*
OS-20628	424.5	BD	5630	60	6280	6200	6000	–	6200*
OS-20632	424.5	BC	5400	40	5930	5910	5900	–	5910
CAMS-70688	449.5	BD	6070	40	6720	6650	6570	–	6650*
CAMS-70689	474.5	BD	7070	40	7680	7670	7590	–	7670*
CAMS-70690	499.5	BD	7220	40	7840	7770	7740	–	7770*
CAMS-69716	506.0	HU§	6690	40	7420	7370	7310	–	7370*
CAMS-69717	506.0	HA§	7050	80	7680	7630	7580	–	7630
CAMS-70691	526.0	BD	7680	40	8330	8270	8180	–	8270*
CAMS-69850	536.0	HU	7800	40	8390	8370	8350	–	8370*
CAMS-70944	536.0	HA	8260	40	9010	8990	8780	–	8990
OS-20614	545.0	BD	8450	50	9270	9180	9030	–	9180*
CAMS-69851	551.0	HU	8410	40	9240	9090	9030	–	9090*
CAMS-69852	551.0	HA	8100	130	8980	8600	8450	–	8600
CAMS-69853	561.0	HU	8780	30	9530	9530	9500	–	9530*
CAMS-69893	561.0	HA	8830	70	9550	9540	9500	–	9540
CAMS-69854	571.0	HU	9190	40	10,190	10,150	9920	–	10,150*
CAMS-69894	571.0	HA	9300	70	10,240	10,220	10,190	–	10,220
CAMS-69855	581.0	HU	9770	40	11,060	11,030	10,690	–	11,030*
CAMS-70945	581.0	HA	10,020	40	11,200	11,190	11,170	–	11,190
OS-26866	586.0	BD	10,080	85	11,260	11,200	11,180	–	11,200*
CAMS-69718	591.0	HU§	10,100	40	11,230	11,230	11,200	–	11,230*
CAMS-69719	591.0	HA§	9900	50	11,170	11,120	10,810	–	11,120
CAMS-71317	606.0	HU	10,210	40	11,550	11,300	11,260	–	11,300*
CAMS-71318	606.0	HA	10,130	40	11,260	11,230	11,200	–	11,230
OS-26867	626.0	BD	10,640	70	12,620	12,330	11,970	–	12,330*
CAMS-71094	631.0	HU	10,790	40	12,830	12,630	12,350	–	12,630*
CAMS-71095	631.0	HA	10,660	50	12,630	12,530	12,110	–	12,530
OS-26868	675.0	BD	11,760	60	13,790	13,460	13,410	–	13,460*
CAMS-71096	683.0	HU	11,990	50	13,840	13,810	13,520	–	13,810*
CAMS-71097	683.0	HA	11,890	60	13,820	13,710	13,460	–	13,710
OS-26869	695.0	BD	12,610	60	15,330	14,320	14,150	–	14,320
CAMS-69720	718.0	HU§	13,100	50	15,680	15,490	14,910	15,490	15,490*
CAMS-69721	718.0	HA§	12,570	50	15,300	14,300	14,140	–	14,300
OS-20615	725.0	BD	13,300	85	15,930	15,690	15,390	15,730	15,730
CAMS-71392	733.0	HU	13,480	50	16,130	15,900	15,680	15,950	15,950*
CAMS-71098	733.0	HA	13,050	40	15,620	15,440	14,570	15,420	15,420
OS-20616	745.0	BD	14,150	95	16,940	16,670	16,430	16,780	16,780
OS-20116	760.0	BD	12,950	55	15,540	15,340	14,430	15,300	15,300
CAMS-69856	783.0	HU	15,680	60	18,730	18,440	18,160	18,640	18,640*
CAMS-70946	783.0	HA	13,270	60	15,890	15,660	15,340	15,700	15,700

Table 2 (*continued*)

Laboratory accession no.	Depth below sediment surface (cm)	Fraction dated	^{14}C age	Error	+ 1s yr BP	Rounded yr BP INTCAL98	− 1s yr BP	Coral calibrated age yr BP	Model age yr BP
CAMS-69857	826.5	HU	18,300	60	21,790	21,450	21,120	21,760	21,760*
CAMS-69895	826.5	HA	13,500	240	16,280	15,930	15,570	15,980	15,980
CAMS-69896	856.5	HA	13,420	170	16,130	15,830	15,530	15,880	15,880
CAMS-69858	856.5	HU	18,270	60	21,760	21,420	21,090	21,720	21,720*
CAMS-69859	896.5	HU	17,670	70	21,060	20,730	20,400	21,020	21,020*
CAMS-69897	896.5	HA	12,060	470	14,300	13,820	13,190	–	13,820
OS-20617	924.5	BD	17,200	95	20,520	20,180	19,860	20,460	20,460

Radiocarbon ages younger than 12,620 ^{14}C yr BP are calibrated using INTCAL98 (Method A; Stuiver et al., 1998; Stuiver and Reimer, 1993; Stuiver and Polach, 1977). Older radiocarbon ages are calibrated using a second-order polynomial equation through the published U/Th–^{14}C coral database (Bard et al., 1998). In the text and figures, calendar ages are denoted "yr BP". A 250-year reservoir-water correction has been made to all dates (Abbott et al., 1997a,b).

BD: bulk decalcified; HU: humin; HA: humate; MF: macrophyte fragments; BC: bulk carbonate.

The box-core (NE98-10BXA) and piston core (NE97-7PC) that comprise core site C90m do not overlap; however, the time gap between the cores is believed to be less than a few hundred years.

§ Humin and humate dates from discrete intervals denoted in Fig. 2.

* Ages used in age model.

leave little doubt that interannual precipitation variability on the Altiplano, metered by the intensity of the SASM, is strongly influenced by El Niño-Southern Oscillation (ENSO) variability in the equatorial Pacific ocean–atmosphere system that teleconnects with the tropical Atlantic/Amazon climate system (Aceituno, 1989; Garreaud, 2000; Vuille et al., 2000).

2. Previous geochronological work

Earlier paleoenvironmental studies of Lake Titicaca generally relied on small numbers of radiocarbon ages from bulk decalcified sediments or macrophyte fragments (Wirrmann and Mourguiart, 1995; Cross et al., 1999, and references therein). These studies presented age models sufficiently accurate for defining Holocene lake-level changes at multi-millennial to millennial timescales. Abbott et al. (1997a,b) used 60 AMS-^{14}C dates on fish scales, gastropod shells, and macrophytes to precisely define the last 3500 years of lake-level history in the small southern basin of Lake Titicaca. In addition, Abbott et al. (1997a,b) identified a 250-year ^{14}C hard-water effect for late Holocene sediments of the small basin using ^{210}Pb geochronometry and paired terrestrial/aquatic radiocarbon ages. The 250-year offset of radiocarbon ages was shown to be nearly constant for the past 3500 years, even during lake lowstands.

Cross et al. (1999) and Baker et al. (2001) defined the timing of late Pleistocene/Holocene lake-level fluctuations using radiocarbon ages derived from bulk decalcified sediment from cores recovered from the deep northern sub-basin of Lake Titicaca. The bulk decalcified organic fraction of most lacustrine sediments is an agglomeration of sub-fractions with multiple origins, variable compositions, and different ages (Mathewes and Westgate, 1980; Nelson et al., 1988). Radiocarbon ages on bulk decalcified sediments represent %C-weighted integrations of all organic sub-fractions, minus the small amount of organic matter hydrolyzed during acid decalcification. Comparison of fraction-specific ages can provide more information if macrophytes are absent from the sediment, and ages of several chemically defined organic sub-fractions may provide the best justification for using bulk decalcified ages to support age models. The humin component of sediments is considered to be chemically immobile over the time period used for radiocarbon dating because of its chemical inertness under acidic and alkaline conditions (< 70,000 years; Hatcher et al., 1985). Radiocarbon ages based on humin residues have not been used extensively for dating lake sediments (Abbott and Stafford, 1996); however, they have been investigated in soils, peats, and organic silts (Cook et al., 1998, and references therein). The humin residue is often determined to be a complex mixture of deposition-age organic matter and older,

Table 3
Raw and calibrated radiocarbon results for all fractions and the corresponding sediment depths for core site C150m

Laboratory accession no.	Depth below sediment surface (cm)	Fraction dated	^{14}C age	Error	+ 1s yr BP	Rounded yr BP INTCAL98	− 1s yr BP	Coral calibrated age yr BP	Model age yr BP
OS-21020	0.5	BD	0	0	100	50	10	–	50*
OS-21021	30.0	BD	1490	45	1260	1170	1080	–	1170*
OS-21022	60.0	BD	2370	40	2150	2120	2010	–	2120*
OS-21023	83.0	BD	3490	40	3470	3470	3400	–	3470*
OS-21026	83.0	HU	3850	40	3970	3890	3830	–	3890*
CAMS-70694	107.4†	BD	4920	30	5460	5400	5320	–	5400*
CAMS-70695	113.6†	BD	5190	40	5710	5660	5610	–	5660*
CAMS-61618	114.3	BD	5170	40	5660	5620	5600	–	5620*
CAMS-61619	114.3	HA	5080	40	5600	5590	5490	–	5590
CAMS-61620	114.3	HU	5120	50	5650	5600	5590	–	5600*
CAMS-61639	114.3	MF	5080	50	5600	5590	5490	–	5590
CAMS-70696	116.9†	BD	5310	40	5890	5860	5740	–	5860*
CAMS-70697	119.9†	BD	5420	30	5930	5920	5910	–	5920*
CAMS-70698	125.4†	BD	5380	50	5930	5910	5770	–	5910*
CAMS-70699	134.6†	BD	5390	40	5930	5910	5890	–	5910*
CAMS-70700	139.9†	BD	5490	40	6170	5970	5930	–	5970*
OS-20098	140.4	BD	5550	55	6170	6100	5950	–	6100*
CAMS-70701	143.3†	BD	5570	40	6170	6060	5990	–	6060*
CAMS-70702	153.9†	BD	5900	40	6470	6430	6360	–	6430*
CAMS-61621	153.9	BD	6060	50	6720	6640	6500	–	6640*
CAMS-61622	153.9	HU	6270	50	6900	6820	6760	–	6820*
CAMS-61640	153.9	MF	4580	80	5030	4870	4830	–	4870*
CAMS-70703	165.9†	BD	6280	40	6900	6820	6760	–	6820*
OS-24101	165.9	BD	5820	50	6410	6370	6300	–	6370**
CAMS-61643	172.4	MF	5370	60	5930	5910	5750	–	5910
CAMS-61641	178.4	MF	5340	60	5910	5890	5750	–	5890
CAMS-69704	191.4	HU§	6630	40	7410	7290	7270	–	7290*
CAMS-69705	191.4	HA§	6550	60	7270	7250	7100	–	7250
OS-20094	200.4	BD	7240	75	7930	7810	7700	–	7810*
CAMS-61623	210.0	BD	7730	50	8360	8230	8190	–	8230*
CAMS-61624	210.0	HA	7660	60	8330	8180	8170	–	8180
CAMS-61625	210.0	HU	7800	50	8390	8370	8340	–	8370*
CAMS-61626	221.9	BD	8430	50	9260	9130	9030	–	9130*
CAMS-61627	221.9	HA	8320	40	9030	9010	9000	–	9010
CAMS-61628	221.9	HU	8490	40	9400	9170	9090	–	9170*
CAMS-61642	221.9	MF	8190	40	8980	8850	8640	–	8850
OS-24102	236.9	BD	8830	45	9550	9540	9530	–	9540*
OS-24103	253.9	BD	9340	50	10,240	10,220	10,210	–	10,220*
OS-20095	260.4	BD	10,050	85	11,230	11,200	11,170	–	11,200*
CAMS-69707	263.2	HU§	9760	40	11,060	10,740	10,690	–	10,740*
CAMS-69706	263.2	HA§	9320	50	10,240	10,220	10,190	–	10,220
CAMS-61629	280.2	BD	10,480	50	12,290	11,790	11,760	–	11,790*
CAMS-61630	280.2	HA	10,420	50	12,100	11,820	11,660	–	11,820
CAMS-61631	280.2	HU	10,710	50	12,790	12,490	12,180	–	12,490*
OS-24104	281.7	BD	10,400	70	12,090	11,750	11,570	–	11,750*
CAMS-61632	303.2	BD	11,030	50	12,950	12,880	12,660	–	12,880
CAMS-61633	303.2	HA	10,870	40	12,880	12,730	12,430	–	12,730
CAMS-61634	303.2	HU	11,310	50	13,150	13,020	12,990	–	13,020*
OS-24105	306.7	BD	10,970	55	12,930	12,860	12,640	–	12,860
OS-24106	314.3	BD	11,250	55	13,140	13,000	12,900	–	13,000
CAMS-71086	329.5	HU	11,530	50	13,390	13,170	13,150	–	13,170*

Table 3 (*continued*)

Laboratory accession no.	Depth below sediment surface (cm)	Fraction dated	^{14}C age	Error	+ 1s yr BP	Rounded yr BP INTCAL98	− 1s yr BP	Coral calibrated age yr BP	Model age yr BP
CAMS-71087	329.5	HA	10,940	40	12,910	12,830	12,640	–	12,830
OS-26860	334.8	BD	12,810	60	15,460	14,650	14,340	15,130	15,130
CAMS-71088	338.1	HU	12,180	60	14,080	13,940	13,820	–	13,940*
CAMS-71089	338.1	HA	11,250	40	13,130	13,000	12,900	–	13,000
CAMS-69709	345.5	HU§	11,970	50	13,840	13,810	13,500	–	13,810*
CAMS-69708	345.5	HA§	11,670	40	13,760	13,420	13,180	–	13,420
CAMS-71927	353.8	HU	11,220	40	13,120	12,990	12,890	–	12,990*
CAMS-61635	356.4	BD	14,550	50	17,390	17,140	16,890	17,270	17,270
CAMS-61636	356.4	HA	13,020	50	15,580	15,410	14,500	15,390	15,390
CAMS-61637	356.4	HU	15,420	50	18,420	18,140	17,870	18,320	18,320*
CAMS-74058	364.8	HU	14,030	50	16,780	16,540	16,310	16,630	16,630*
CAMS-74059	364.8	HA	12,130	70	14,060	13,840	13,670	–	13,840
OS-24107	367.3	BD	14,350	65	17,160	16,910	16,660	17,020	17,020
CAMS-71928	370.3	HU	10,710	40	12,790	12,490	12,180	–	12,490*
CAMS-74060	372.8	HU	14,080	70	16,840	16,590	16,360	16,690	16,690*
CAMS-74061	372.8	HA	12,370	120	15,140	14,110	13,850	–	14,110
CAMS-71929	378.3	HU	10,390	40	11,950	11,720	11,580	–	11,720*
CAMS-61638	380.1	BD	15,660	60	18,710	18,410	18,140	18,610	18,610
CAMS-74062	387.1	HU	14,020	50	16,760	16,530	16,300	16,620	16,620*
CAMS-71930	391.1	HU	13,170	60	15,770	15,550	15,120	15,570	15,570*
CAMS-71931	411.1	HU	14,570	60	17,420	17,160	16,910	17,290	17,290*
CAMS-74063	419.1	HU	13,630	50	16,310	16,080	15,850	16,140	16,140*
CAMS-74513	435.1	BD	16,530	50	19,730	19,410	19,110	19,660	19,660
CAMS-74064	435.1	HU	15,330	50	18,310	18,030	17,770	18,210	18,210*
CAMS-71932	436.1	HU	16,090	70	19,220	18,910	18,610	19,130	19,130*
OS-20096	439.1	BD	17,200	50	20,510	20,180	19,870	20,460	20,460
CAMS-74065	451.1	HU	14,710	50	17,580	17,320	17,070	17,460	17,460*
CAMS-74066	459.1	HU	16,450	50	19,630	19,320	19,020	19,560	19,560*
CAMS-71933	496.1	HU	15,190	60	18,150	17,870	17,610	18,050	18,050*
CAMS-74514	509.6	BD	15,440	50	18,440	18,160	17,890	18,350	18,350
CAMS-74067	509.6	HU	14,420	50	17,240	16,990	16,750	17,110	17,110*
OS-20097	521.6	BD	18,900	170	22,540	22,140	21,760	22,460	22,460
CAMS-74068	525.6	HU	16,400	50	19,580	19,260	18,960	19,500	19,500*
CAMS-74069	525.6	HA	11,920	100	13,830	13,690	13,460	–	13,690
CAMS-74848	541.6	HU	16,020	60	19,130	18,830	18,540	19,050	19,050*
CAMS-74070	541.6	HA	11,410	70	13,180	13,150	13,020	–	13,150
CAMS-74071	557.6	HU	15,060	50	17,990	17,720	17,470	17,890	17,890*
CAMS-74072	557.6	HA	10,010	100	11,230	11,180	11,120	–	11,180
CAMS-71934	581.6	HU	16,810	60	20,060	19,740	19,430	19,990	19,990*
CAMS-74515	597.6	BD	18,730	50	22,300	21,950	21,610	22,260	22,260
CAMS-74073	597.6	HU	17,400	60	20,740	20,410	20,090	20,700	20,700*
CAMS-74074	597.6	HA	13,790	90	16,510	16,260	16,020	16,340	16,340
OS-20099	686.1	BD	20,900	190	pc	pc	pc	24,780	24,780
CAMS-74516	688.1	BD	20,550	60	pc	pc	pc	24,370	24,370
CAMS-74075	688.1	HU	18,720	60	22,290	21,930	21,600	22,250	22,250*
CAMS-74076	688.1	HA	14,820	70	17,720	17,450	17,190	17,600	17,600
CAMS-74077	784.1	HU	20,440	70	23,910	23,910	23,520	24,250	24,250*
CAMS-74078	784.1	HA	15,790	90	18,870	18,560	18,270	18,770	18,770
CAMS-74517	828.1	BD	22,800	70	pc	pc	pc	26,930	26,930
CAMS-74079	828.1	HU	22,100	80	pc	pc	pc	26,140	26,140*
CAMS-74080	828.1	HA	17,530	100	20,910	20,560	20,230	20,850	20,850

(continued on next page)

Table 3 (*continued*)

Laboratory accession no.	Depth below sediment surface (cm)	Fraction dated	^{14}C age	Error	+ 1s yr BP	Rounded yr BP INTCAL98	− 1s yr BP	Coral calibrated age yr BP	Model age yr BP
OS-10384	872.1	BD	23,400	250	pc	pc	pc	27,600	27,600
CAMS-74081	908.1	HU	21,350	80	pc	pc	pc	25,290	25,290*
CAMS-74082	908.1	HA	17,880	100	21,320	20,970	20,630	21,260	21,260
CAMS-74518	983.1	BD	25,990	100	pc	pc	pc	30,460	30,460
CAMS-74083	983.1	HU	24,420	100	pc	pc	pc	28,740	28,740*
CAMS-74084	983.1	HA	20,140	90	23,980	23,570	23,180	23,900	23,900
CAMS-74085	1095.1	HU	24,490	100	pc	pc	pc	28,810	28,810*
CAMS-74086	1095.1	HA	21,560	160	pc	pc	pc	25,530	25,530

Because subcentimeter-scale correlation of laminations between the two core sites is possible, the mid-Holocene radiocarbon geochronology developed for the BMC core was imported into the C150m radiocarbon geochronology. Radiocarbon ages from the BMC core are reported with the corresponding depth from core site C150m.

(pc): "pre-calibration", indicating that the radiocarbon date is beyond the range of INTCAL98 calibration routine. The bottom 18.7 cm of box-core NE98-4BXB is visibly/geochemically correlative to the top 18.7 cm of piston core NE98-1PC, thus a complete record of sedimentation is represented for core site C150m.

* Ages used in age model.

** The large incoherency between this date and dates from nearby intervals in core sites C150m and BMC resulted in the exclusion of this date from the age model.

† Piston core BMC, recovered in the vicinity of core site C150m (see Fig. 1b), is currently being used for detailed studies of organic biomarkers and mid-Holocene organic/inorganic carbon sedimentation.

§ Humin and humate dates from discrete intervals denoted in Fig. 2.

recalcitrant, redeposited material, much of which is potentially locked up in clays (Schoute et al., 1983; Blystad and Selsing, 1989; Lowe, 1991, and references therein).

Under certain circumstances wherein the humin sub-fraction is known to include carbon from older sources, the age of the humate sub-fraction may be more accurate (Head et al., 1989, and references therein). However, the mobility of humates through soil and sediment profiles over geologic time is well-documented (Wassenaar et al., 1990, and references therein), and the validity of constructing age models using ages derived from humate over those from humin must be critically evaluated for each chronology (Shore et al., 1995). A more detailed geochronological investigation of Lake Titicaca sediment cores (Rowe et al., 2002) showed that, although the Holocene portion of the age model constructed by Baker et al. (2001) is sound, the possibility of post-depositional mobility of certain organic fractions may result in several internally consistent age models for late-Pleistocene sediments. The present study seeks to refine the chronology of late Quaternary lake-level fluctuations that are intimately linked to fluctuations in moisture transport to the Altiplano and large-scale, long-term shifts in tropical hydrologic balance. Here, we introduce 125 new ^{14}C dates on three different sediment fractions from three cores from the deep basin to improve the overall geochronology and to better characterize late Pleistocene age inaccuracies.

3. Methods

Samples for radiocarbon analysis were collected from three core sites (C90m, C150m, C230m) (Fig. 1b; Table 1) in the deep, northern sub-basin of the lake. Core sites were chosen to reflect a range in water depth (90–230 m) corresponding to a range in depositional sub-environment. We focused on dating chemically separable organic fractions because macrofossils were largely absent from our cores. We separated and analyzed the bulk decalcified sediment, humate (base-soluble, acid-insoluble), and humin (acid/base insoluble) sedimentary constituents. Laboratory sample preparation included drying bulk sediments at 60 °C followed by grinding in a mortar and pestle. Pre-weighed samples were acidified (1 N HCl) at 90 °C to remove carbonate. The resulting bulk decalcified fraction was rinsed with deionized water until neutral. An aliquot of bulk decalcified material was reacted with 1 N NaOH at 90 °C to separate the

Table 4
Raw and calibrated radiocarbon results for all fractions and the corresponding sediment depths for core site C230m

Laboratory accession no.	Depth below sediment surface (cm)	Fraction dated	^{14}C age	Error	+ 1s yr BP	Rounded yr BP INTCAL98	− 1s yr BP	Coral calibrated age yr BP	Model age yr BP
CAMS-71319	70.0	HU	3050	40	2950	2910	2850	–	2910*
CAMS-71320	70.0	HA	2790	40	2740	2730	2510	–	2730
OS-17703	83.0	BD	3650	30	3690	3670	3590	–	3670*
CAMS-71321	108.5	HU	4790	40	5310	5290	5050	–	5290*
CAMS-71322	108.5	HA	4740	40	5290	5110	5040	–	5110
CAMS-71323	133.5	HU	5420	40	5980	5920	5910	–	5920*
CAMS-71324	133.5	HA	5350	40	5910	5890	5750	–	5890
OS-20114	140.5	BD	5510	45	6170	5990	5940	–	5990*
OS-20610	145.5	BD	6540	40	7260	7250	7160	–	7250*
CAMS-71325	163.5	HU	6320	40	6990	6900	6810	–	6900*
CAMS-71326	163.5	HA	6340	40	7000	6910	6810	–	6910
OS-20611	185.5	BD	7750	110	8390	8340	8180	–	8340*
CAMS-69710	193.5	HU§	6720	50	7430	7370	7320	–	7370*
CAMS-69711	193.5	HA§	6770	50	7460	7430	7340	–	7430
OS-26870	225.5	BD	7820	45	8400	8380	8350	–	8380*
CAMS-69860	238.5	HU	8350	40	9060	9010	9010	–	9010*
CAMS-69898	238.5	HA	8420	60	9260	9090	9030	–	9090
OS-26871	275.0	BD	9120	45	10,150	10,020	9870	–	10,020*
CAMS-69861	293.0	HU	9870	40	11,160	10,920	10,790	–	10,920*
CAMS-70947	293.0	HA	10,000	40	11,200	11,180	11,170	–	11,180
CAMS-69712	308.0	HU§	9980	50	11,200	11,170	11,160	–	11,170*
CAMS-69713	308.0	HA§	9720	50	11,040	10,690	10,600	–	10,690
OS-20612	315.0	BD	10,400	55	12,090	11,750	11,580	–	11,750*
CAMS-69862	358.0	HU	11,040	40	12,950	12,890	12,660	–	12,890*
CAMS-70948	358.0	HA	10,960	50	12,920	12,850	12,640	–	12,850
OS-26872	365.0	BD	11,270	55	13,140	13,010	12,910	–	13,010
CAMS-71092	378.0	HU	12,020	40	13,850	13,820	13,600	–	13,820*
CAMS-71093	378.0	HA	11,670	60	13,760	13,420	13,180	–	13,420
CAMS-69863	401.5	HU	12,870	50	15,490	14,580	14,370	15,200	15,200*
CAMS-69899	401.5	HA	12,350	50	15,090	14,100	13,850	–	14,100
OS-26873	418.5	BD	13,290	80	15,920	15,680	15,370	15,720	15,720
CAMS-69714	421.5	HU§	13,370	50	16,000	15,770	15,530	15,820	15,820*
CAMS-69715	421.5	HA§	12,800	60	15,450	14,670	14,330	15,110	15,110
CAMS-71327	426.5	HU	14,300	50	17,090	16,850	16,610	16,960	16,960*
CAMS-71328	426.5	HA	13,020	40	15,580	15,410	14,500	15,390	15,390
CAMS-71329	431.5	HU	14,700	50	17,570	17,310	17,060	17,450	17,450*
CAMS-71330	431.5	HA	12,960	50	15,550	15,350	14,430	15,310	15,310
CAMS-71393	436.5	HU	16,250	50	19,400	19,090	18,800	19,320	19,320*
CAMS-71331	436.5	HA	13,100	40	15,680	15,490	14,920	15,490	15,490
CAMS-69864	441.5	HU	16,860	40	20,110	19,790	19,490	20,050	20,050*
CAMS-70949	441.5	HA	13,210	40	15,810	15,580	15,220	15,620	15,620
OS-26874	478.5	BD	15,810	90	18,900	18,590	18,290	18,790	18,790
CAMS-69865	478.5	HU	18,650	50	22,200	21,850	21,520	22,170	22,170*
CAMS-69900	481.5	HA	13,280	60	15,900	15,670	15,360	15,710	15,710
OS-20613	514.5	BD	17,450	80	20,810	20,470	20,150	20,750	20,750
CAMS-69866	521.5	HU	20,650	80	pc	pc	pc	24,490	24,490*
CAMS-69901	521.5	HA	13,210	130	15,850	15,580	15,170	15,620	15,620
CAMS-69867	563.0	HU	18,690	60	22,250	21,900	21,560	22,220	22,220*
CAMS-70950	563.0	HA	14,820	210	17,800	17,450	17,110	17,600	17,600
CAMS-69868	598.0	HU	21,230	80	pc	pc	pc	25,150	25,150*

(continued on next page)

Table 4 (*continued*)

Laboratory accession no.	Depth below sediment surface (cm)	Fraction dated	^{14}C age	Error	+ 1s yr BP	Rounded yr BP INTCAL98	− 1s yr BP	Coral calibrated age yr BP	Model age yr BP
CAMS-70951	598.0	HA	15,400	130	18,430	18,110	17,820	18,300	18,300
CAMS-69869	633.0	HU	21,320	70	pc	pc	pc	25,260	25,260*
CAMS-70952	633.0	HA	15,590	430	18,910	18,330	17,780	18,530	18,530
CAMS-69870	673.0	HU	20,690	80	pc	pc	pc	24,540	24,540*
CAMS-69902	673.0	HA	14,340	230	17,250	16,890	16,550	17,010	17,010
CAMS-69871	714.0	HU	20,750	60	pc	pc	pc	24,600	24,600*
CAMS-69903	714.0	HA	14,430	190	17,330	17,000	16,680	17,120	17,120
CAMS-69872	749.0	HU	22,680	80	pc	pc	pc	26,800	26,800*
CAMS-69937	749.0	HA	15,500	550	18,930	18,230	17,550	18,420	18,420
CAMS-69873	789.0	HU	22,570	90	pc	pc	pc	26,670	26,670*
CAMS-70953	789.0	HA	17,040	100	20,340	20,000	19,670	20,270	20,270

Because core site C230m does not incorporate a box core, the depth below sediment surface represented by the top of C230m is estimated by visually and geochemically comparing C230m with C150m.

* Ages used in age model.

§ Humin and humate dates from discrete intervals denoted in Fig. 2.

humate and humin fractions. Following repeated additions of base and sequential removal of the humate fraction, the humin residue was acidified (1 N HCl, 90 °C) and then rinsed three times with deionized water. The humate fraction was precipitated with concentrated HCl and rinsed three times with deionized water. Following rinsing, all fractions were vacuum-dried, combusted and graphitized. Samples were analyzed at the Center for Accelerator Mass Spectrometry at Lawrence Livermore National Laboratory and at the NOSAMS facility at Woods Hole Oceanographic Institution (Tables 2–4).

4. Results: comparison of ages from multiple cores

All bulk decalcified, humate, and humin ages are tabulated in Tables 2–4. In order to show preliminary inter- and intra-fraction age patterns within and between cores, down-core bulk geochemical records

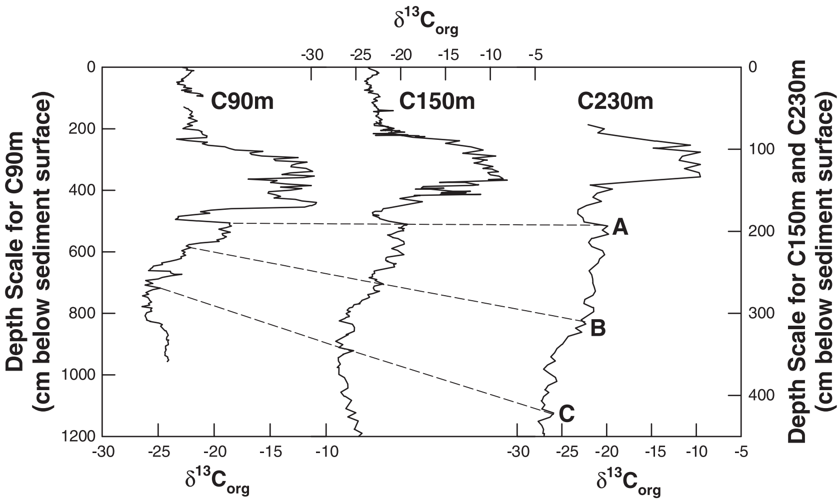

Fig. 2. Down-core stable isotopic records of bulk organic carbon ($\delta^{13}C_{org}$) from piston cores recovered from the three core sites were used along with C/N (not shown) to identify three intervals of similar age. The chosen intervals are connected by dashed lines and denoted “A”, “B”, and “C”. Humate and humin fractions for each interval in each core were radiocarbon dated and are denoted by ‘§’ in Tables 2–4.

were utilized to identify three discrete, correlative intervals to date in the three piston cores (Fig. 2). Age results for the three intervals, denoted "A", "B", and "C" in Fig. 2, are indicated by '§' in Tables 2–4. The results suggest that within an interval, (1) ages derived from humin have a smaller age range than ages derived from humate, and (2) with only one exception, humate ages are younger than their corresponding humin ages. The preliminary results suggest

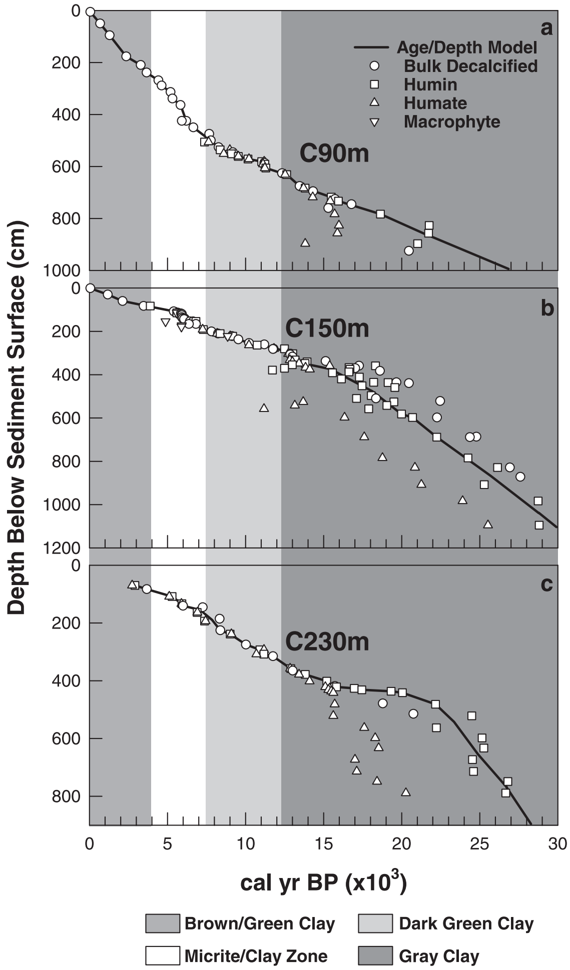

Fig. 3. Down-core bulk decalcified, humate, and humin age results for the three core sites: (a) C90m, (b) C150m, (c) C230m, plotted with respect to calendar age, sediment depth below surface, and a simplified stratigraphy. Solid lines indicate the model used to assign ages to down-core results. Age models are based upon ages from bulk decalcified and humin (humin) sub-fractions in the post-13,500 yr BP (pre-13,500 yr BP) interval.

that humin residues give more coherent ages between cores for a given sedimentary interval.

Ages are presented for each core site in the context of sediment depth and stratigraphy (Fig. 3). The age/depth curves for each fraction in each core are generally consistent down-core, and ages derived from any of the three organic fractions are generally coherent in sediments younger than 13,500 yr BP. In the pre-13,500 yr BP interval, however, ages of the various fractions are divergent, with age offsets as large as 7000 years for a given interval. At sites C90m and C230m, humate ages are consistently youngest, followed by bulk decalcified ages and humin ages (oldest), heretofore denoted the "HA–BD–HU" age pattern. At the intermediate water depth core site, C150m, humate ages are consistently youngest, followed by humin ages and bulk decalcified ages (oldest), heretofore denoted the "HA–HU–BD" age pattern.

5. Discussion

5.1. Between-core and between-fraction age inhomogeneity

Differences in depositional sub-environment create between-core incoherencies in age, geological signature, and proxy record signature that are revealed when comparing multiple down-core records from the same lake. These incoherencies arise from differences in sedimentation rate, bioturbation, pelagic versus littoral input, and detrital input. With the exception of the sample chosen for interval "C" at core site C150m, we believe the minor within-fraction age differences for the three discrete intervals in Fig. 2 are predominantly a consequence of the depositional inhomogeneity between the respective core sites. We believe the sample chosen for interval "C" at core site C150m does not represent the same discrete interval chosen for the other two core sites.

In Lake Titicaca sediments, age consistency between different organic fractions in the post-13,500 yr BP sediment interval affirms the use of any or all chemically extractable sub-fractions, including the bulk decalcified fraction, for constructing age/depth models possessing centennial-scale accuracy. This is not the case for the pre-13,500 yr BP interval, within

which humate, bulk decalcified, and humin ages from a discrete sample interval may span several thousand years (Fig. 3). The HA–BD–HU age pattern observed at core sites C90m and C230m suggests that these sediments underwent a similar depositional and/or post-depositional history that was different from that of core site C150m. Mass balance calculations using the organic fractions of C230m (not shown) indicate the bulk decalcified fraction is predominantly a mixture of humin and humate sub-fractions. This cannot be the case for core site C150m, characterized by a bulk decalcified fraction that is older than both humin and humate sub-fractions. The HA–HU–BD age pattern of core site C150m implies that the bulk decalcified fraction integrates an older sub-fraction that is hydrolyzed during base extraction but is not re-precipitated during the humate recovery step (addition of concentrated HCl). As a consequence, this alkali-mobile, acid-soluble sub-fraction does not contribute to the humate or humin age results. Furthermore, because this sub-fraction initially hydrolyzes under basic conditions and does not re-precipitate during acidification, it is by definition a fulvic sub-component (e.g., Rashid and King, 1970), which we designate here as the "Alkali-Mobile Fulvic" or AMF sub-fraction.

The solubility properties and greater age of the AMF sub-fraction make it inherently different from the humin and humate sub-fractions. The AMF sub-fraction is not removed during initial sediment decalcification revealing that its origin and/or chemical stability is different from other fulvic acids that are released during the decalcification step. This observation leads us to propose a group of mechanisms that stabilize or "protect" the AMF sub-fraction from hydrolyzing during the initial decalcification step, but permanently destabilize the AMF sub-fraction during the subsequent alkaline treatment. We believe the most suitable set of circumstances under which otherwise-mobile organics are sequestered from solution is through organic–mineral and/or organo–metallic interactions, or through simple occlusion of organics within mineral pore spaces.

5.2. Potential mechanisms that stabilize/destabilize the AMF sub-fraction

We believe the AMF sub-fraction inferred from the HA–HU–BD age pattern at core site C150m has its origins through one or several mechanism(s): organic adsorption on mineral surfaces, organo–metallic interactions, occlusion of organic matter into sealed mineral pore spaces, or interlamellar binding (adsorption/absorption) of fulvic/humic molecules (Schnitzer and Kodama, 1967; Rashid and King, 1970; Greenland, 1971; Rashid, 1971; Rashid et al., 1972; Davis and Gloor, 1981; Davis, 1982; Preston and Riley, 1982; Jardine et al., 1989; Wang and Lee, 1993; Gu et al., 1994, 1995; Kiel et al., 1994; Thimsen and Kiel, 1998; Hedges and Kiel, 1999; Arnarson and Kiel, 2000). Some mechanisms are better at sequestering the AMF sub-fraction than others, and certainly some mechanisms do not uniquely apply to core site C150m. We believe the origin of the AMF sub-fraction is reasonably explained if eroded clays containing radiocarbon-depleted organic matter (fulvic acids) within their interlamellar sites were deposited at core site C150m but did not represent a significant depositional component at the other two core sites. The initial decalcification step may extract some of the fulvics held in the interlamellar sites, but much of this sub-fraction remains immobilized. In addition to the humate fraction, the alkaline hydrolysis liberates most of the interlamellae-bound fulvic fraction, which remains in suspension during the subsequent re-acidification.

Why might core site C150m receive clays containing interlamellae-bound carbon and not the other two core sites? A difference in source materials may account for this differential sedimentation pattern. Because of its location in Yunguyo Bay, core site C150m may have received a significant portion of its glacial clays from the weathered and glaciated volcanic terrain exposed around the southern portion of Lago Grande. Core site C90m most likely received most of its input from the sedimentary strata (predominantly red sandstones) on the western edge of the lake, and core site C230m likely received its glacial inputs directly from the sedimentary strata and granitic complexes exposed in the eastern cordillera. In addition to interlamellar mechanisms, strong mineral surface sorption, organo–metallic complexation, and/or pore space occlusion of organic constituents potentially explain the reason for the HA–HU–BD age pattern at C150m, but it is difficult to rationalize why these same mechanisms would not be important at

core sites C90m and C230m. A detailed investigation of mineral content and provenance would help decipher the sedimentological differences between the core sites.

5.3. Suitability of the various fractions for constructing age models in the pre-13,500 yr BP interval

Regardless of core location, the youngest extractable organic component in the pre-13,500 yr BP interval is the humate sub-fraction. The younger age of the humate sub-fraction and the significant age difference between the humin and humate components most likely reflect the downward movement of humate through interconnected pore spaces (Wassenaar et al., 1990, and references therein). The solubility of the AMF sub-fraction under alkaline/acidic conditions also characterizes it as a mobile component over geologic time, rendering it unfavorable for age dating purposes. Bulk decalcified ages integrate the humate and AMF sub-fractions, suggesting the bulk decalcified fraction may not be the most suitable fraction to use for constructing age models in sediments prior to 13,500 yr BP. Given this, the humin sub-fraction is apparently the optimal component for age-dating at all core sites in Lake Titicaca. Humin is insoluble over geologic time and the organic-poor Altiplano soils create a low potential for input of old detrital (not interlamellae-bound) carbon from the surrounding basin (Binford et al., 1992; Rodrigo and Wirrmann, 1992). In addition, the bulk C/N ratio of glacial age sediments (C/N < 6) does not reflect a significant terrestrial input of organic matter (C/N>40). Down-core wt.% C_{org}, C/N, and $\delta^{13}C_{org}$ records are plotted to illustrate core-to-core reproducibility within the post-13,500 yr BP interval, and the effectiveness of using the humin fractions for obtaining ages that best represent depositional ages in the pre-13,500 yr BP interval (Fig. 4a–c).

The geochronologies between core sites are slightly diachronous in the middle Holocene interval. In these laminated, carbonate-rich facies, interpreted to represent mid-Holocene lowstand deposits, isotopic and chemical variability at the shallow water core site leads changes at the intermediate and deep water core sites by approximately 500–800 years. Seismic profiles of the lake sediments (Seltzer et al., 1997) indicate that the mid-Holocene lake level reached 85 m below modern. This interpretation brings the shallow water core site within ∼ 5 m of the mid-Holocene shoreline. Given the near-shore setting of core site C90m during the mid-Holocene and the certainty of erosion of exposed lakebed above the core site, organic deposition at the shallow water core site was probably a mixture of "new" organic carbon and slightly older, eroded material. Accordingly, sediments in the mid-

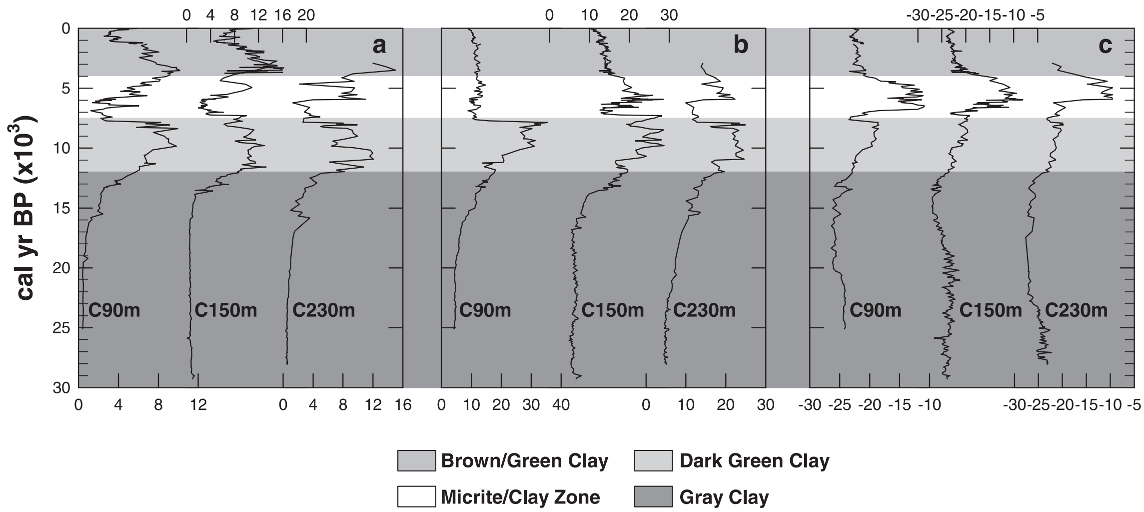

Fig. 4. Down-core (a) wt.% C_{org}, (b) C/N, and (c) $\delta^{13}C_{org}$ results for all core sites. A simplified stratigraphy is also shown for each plot.

Holocene section of the shallow water core site appear slightly older than sediments at the intermediate and deep water core sites, which did not receive significant eroded organic matter.

5.4. Timing of lake level change and global climate change

The down-core isotopic composition of bulk organic carbon ($\delta^{13}C_{org}$) from the deep water core site is plotted with an age model based on eight bulk decalcified and nine humin ages in the post-13,500 yr BP interval and 16 humin ages from the pre-13,500 yr BP interval (Fig. 5). $\delta^{13}C_{org}$ records relative shifts between lighter isotopic signatures associated with pelagic algae (~ -24‰) and heavier isotopic signatures of littoral zone macrophytes ($\sim -12 \pm 4$‰) found in the lake shallows (Cross et al., 1999; Baker et al., 2001; Rowe et al., 2002). Consequently, down-core $\delta^{13}C_{org}$ changes with shoreline proximity to core site, and in essence represents late Quaternary changes in the level of Lake Titicaca. Plotted along with the proxy lake-level record are ice-core $\delta^{18}O$ and δD records from a nearby icecap (Sajama; Thompson et al., 1998), the Greenland Icecap (GISP2; Grootes et al., 1993), and two Antarctic icecaps (Vostok, Jouzel et al., 1996; Taylor Dome, Steig et al., 1998) (Fig. 5). Isotopic changes in the ice cores reflect large-scale changes in hemispheric and global climate.

Fig. 5 illustrates that highstand conditions existed at Lake Titicaca during most of the last glacial episode. According to the $\delta^{13}C_{org}$ proxy, a multi-millennial regressive phase began during or just prior to the Bølling/Allerød period, and continued into the Pre-Boreal period. The decrease in lake level is probably in response to a weakening of the SASM,

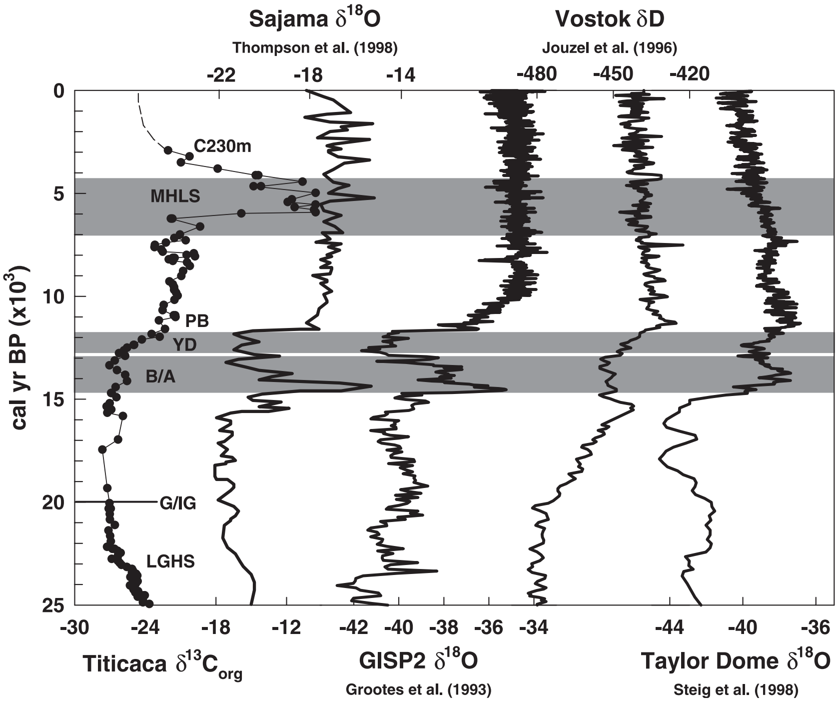

Fig. 5. Down-core $\delta^{13}C_{org}$ curve from C230m plotted alongside ice-core $\delta^{18}O$ and δD records from a nearby icecap (Sajama), the Greenland Icecap (GISP2), and two Antarctic icecaps (Vostok, Taylor Dome). The $\delta^{13}C_{org}$ curve is interpreted as a record of lake level, by which highstands (lowstands) are characterized by more (less) depleted $\delta^{13}C_{org}$, respectively. The last 3000 years of the $\delta^{13}C_{org}$ record, represented by the dotted line, is inferred using results from other core sites. LGHS: Last Glacial Highstand; G/IG: Glacial/Interglacial; B/A: Bølling/Allerød; YD: Younger Dryas; PB: Pre-Boreal; MHLS: Mid-Holocene Lowstand. The Glacial/Interglacial boundary denotes when alpine glaciers are thought to have receded on the northern Altiplano, determined by a significant decrease in down-core magnetic susceptibility (Seltzer, personal communications).

a consequence of decreased summer insolation to the southern hemisphere. The weakening of the SASM across the Pleistocene–Holocene boundary was out of phase with the strengthening West African monsoon, a response to increased northern hemisphere insolation (deMenocal et al., 2000b).

At the submillennial timescale, the $\delta^{13}C_{org}$-based lake-level reconstruction of the Bølling/Allerød to Pre-Boreal period is inconsistent with a previously published diatom-based lake-level record from Lake Titicaca (Baker et al., 2001), although we believe the discordance in interpretations is not a function of different geochronologies, but instead, arises from differences in proxy response to internal lake processes, and to a lesser degree, proxy-specific diagenetic effects, and proxy calibration. The diatom-based lake-level record indicates changes in water depth beginning in the Bølling/Allerød period, but inferences based on the diatom data suggest a series of oscillations in lake level in the period from about 15,000 to 8000 yr BP, in contrast to the more directional pattern evident in the $\delta^{13}C_{org}$. Modern data from Lake Titicaca indicate that both $\delta^{13}C_{org}$ (Cross et al., 1999; Rowe et al., 2002) and diatom abundance patterns (Tapia et al., manuscript in preparation) show clear relationships to lake depth, and the strength of these relationships supports the use of both proxies as indicators of lake-level change. The differences in pattern of the two proxies during deglaciation likely reflect differences in the thresholds for response to lake-level change and variables affected by lake-level change. Thus, as the elevation of Lake Titicaca fluctuated above and below the outlet level in response to climate variation, the timing and rate of response of the physico-chemical variables that affect diatoms were not identical to the timing and rate of change in the factors that produced changes in $\delta^{13}C_{org}$. In any case, it is clear that a distinct lake-level response to insolation change during deglaciation began during or just prior to the Bølling/Allerød period.

Lake level dropped precipitously during the middle Holocene by approximately 85 m, as inferred from ostracode biostratigraphy and seismic stratigraphy (Wirrmann and Mourguiart, 1995, and references therein; Seltzer et al., 1997). The mid-Holocene lowstand (MHLS) at Lake Titicaca is the most obvious climate episode of the last 25,000 years, yet, with the exception of the post-6000 yr BP variability increase in the $\delta^{18}O$ profile of the Sajama record, the MHLS is not reflected by substantial changes in the ice-core records. This suggests that ice-core records from the interior of Greenland and Antarctica were largely insensitive to the variables that forced the mid-Holocene regressive phase at Lake Titicaca. However, recent evidence from the Palmer Deep, immediately west of the Antarctic Peninsula, indicates that the middle Holocene was a time of significantly increased surface productivity (Domack et al., 2001), perhaps brought about by a strong teleconnection to sustained El Niño-Southern Oscillation (ENSO) warm mode conditions. The MHLS is thought to be a non-linear coupled response to ENSO and insolation (Martin et al., 1993; Rowe et al., 2002), as it is nearly concurrent with the mid-Holocene re-establishment of ENSO conditions in the equatorial Pacific (Sandweiss et al., 2001, and references therein). The shift toward a strengthened SASM (and weakened West African monsoon) occurred between 5000 and 6000 yr BP. The subsequent transgressive phase, leading to modern lake highstand conditions, began as early as 5000 yr BP.

6. Conclusions

The timing of continent-scale and interhemispheric paleoenvironmental changes can only be as accurate as the geochronological underpinnings of the individual records. Often, the weakest aspect of a paleoenvironmental reconstruction is the age control. The results presented here indicate various pitfalls associated with reliance upon a single core site and a single organic fraction for dating purposes. We have established what we believe is the optimal fraction for constructing an age model for Lake Titicaca that most accurately reflects the age of sediment deposition by comparing radiocarbon ages of chemically defined organic fractions from multiple core sites. Radiocarbon ages derived from bulk decalcified sediment, humate, and humin fractions generally agree within standard AMS-^{14}C errors of $\sim$ 50–80 years for sediments deposited after 13,500 yr BP. Internally consistent chronologies can be developed using bulk decalcified sediment and humate fractions. However, on the basis of mobility, we believe these fractions do not yield the most representative ages for deposition

in the pre-13,500 yr BP interval. Because of the presumably insignificant input of old detrital carbon (with the exception of mid-Holocene sedimentation to C90m) and the geochemically inert nature of the acid/alkali-insoluble residue we selected the humin subfraction to establish core chronology in this analysis, especially in pre-13,500 yr BP sediments.

We used down-core geochemical proxy results to define large-scale changes in the level of Lake Titicaca during the past ~ 29,000 years. Comparison of the lake-level record with isotopic profiles from ice cores reveals that the middle Holocene lowstand present at Lake Titicaca is absent in polar ice cores and the Sajama ice core. In the Sajama core it marks the onset of more variable $\delta^{18}O$. Over a multi-millennial time scale the Lake Titicaca record is consistent among the different lake-level proxies, but in finer detail we must further consider how internal lake processes, post-depositional effects, and the limitations of modern site calibration influence the interpretation of individual proxies. In addition to strengthening the Lake Titicaca record for use as a regional paleohydrology index, the geochronological refinement presented here permits stronger paleoclimate comparisons to be established between the central Andes and distant records of global change.

Acknowledgements

This work was supported by the University of California's Center for Accelerator Mass Spectrometry minigrant, NSF funding to R. Dunbar (ATM9896152) and G. Seltzer (ATM9708258), and a Stanford University McGee Fund grant to H. Rowe. We sincerely thank Matt Grove and Pedro Tapia for field assistance and discussions, and we deeply value the assistance of Brian Frantz and Paula Zermeño (CAMS-LLNL). The coring and post-coring support of James Broda and Parker Hackett (Woods Hole Oceanographic Institution), the general support of Jorge Calvo and Alfredo de La Paz (USAID, Bolivia), and the warm friendship and support of the Ando Family are deeply valued. We also thank Mark Bush (Florida Institute of Technology) for providing several radiocarbon ages from C150m, and we greatly appreciate the efforts of Ing. Julio Sanjines and Ing. Mario Revollo (Autoridad Autonoma de Lago Titicaca), Nicolas Catari and Gonzalo Mollenzon. Radiocarbon analyses were performed under the auspices of the U.S. Department of Energy by the University of California's Lawrence Livermore National Laboratory (contract W-7405-Eng-48). We deeply appreciate the editorial comments of Mark Abbott and Lisa Sloan.

References

Abbott, M.B., Stafford, T.W., 1996. Radiocarbon geochemistry of modern and ancient Arctic lake systems, Baffin Island, Canada. Quat. Res. 45, 300–311.

Abbott, M.B., Binford, M.W., Brenner, M., Kelts, K.R., 1997a. A 3500 ^{14}C yr high-resolution record of water-level changes in Lake Titicaca, Bolivia/Peru. Quat. Res. 47, 169–180.

Abbott, M.B., Seltzer, G.O., Kelts, K.R., Southon, J., 1997b. Holocene paleohydrology of the tropical Andes from lake records. Quat. Res. 47, 70–80.

Aceituno, P., 1989. On the functioning of the Southern Oscillation in the South American sector: Part II. Upper-air circulation. J. Clim. 2, 341–355.

Arnarson, T.S., Kiel, R.G., 2000. Mechanisms of pore water organic matter and adsorption to montmorillonite. Mar. Chem. 71, 309–320.

Baker, P.A., Seltzer, G.O., Fritz, S.C., Dunbar, R.B., Grove, M.J., Tapia, P.M., Cross, S.L., Rowe, H.D., Broda, J.P., 2001. The history of South American tropical precipitation for the past 25,000 years. Science 291, 640–643.

Bard, E., Arnold, M., Hamelin, B., Tisnerat-Laborde, N., Cabioch, G., 1998. Radiocarbon calibration by means of mass spectrometric $^{230}Th/^{234}U$ and ^{14}C ages of corals. An updated database including samples from Barbados, Mururoa, and Tahiti. Radiocarbon 40 (3), 1085–1092.

Binford, M.W., Brenner, M., Engstrom, D.R., 1992. Temporal sedimentation patterns in the nearshore littoral of Lago Huiñaimarca. In: Dejoux, C., Iltis, A. (Eds.), Lake Titicaca. A Synthesis of Limnological Knowledge. Kluwer Academic Publishing, Dordrecht, The Netherlands, pp. 29–39.

Blystad, P., Selsing, L., 1989. Some erroneous radiocarbon dates of lacustrine sediments. Nor. Geol. Tridskr. 69, 201–208.

Cook, G.T., Dugmore, A.J., Shore, J.S., 1998. The influence of pretreatment of humic acid yields and ^{14}C age of *Carex* peat. Radiocarbon 40 (1), 21–27.

Cross, S.L., Baker, P.A., Seltzer, G.O., Fritz, S.C., Dunbar, R.B., 1999. A new estimate of the Holocene lowstand level of Lake Titicaca, and implications for tropical paleohydrology. Holocene 10, 21–32.

Davis, J.A., 1982. Adsorption of natural dissolved organic matter at the oxide/water interface. Geochim. Cosmochim. Acta 46, 2381–2393.

Davis, J.A., Gloor, R., 1981. Adsorption of dissolved organics in lake water by aluminum oxide. Effect of molecular weight. Environ. Sci. Technol. 15 (10), 1223–1229.

deMenocal, P., Ortiz, J., Guilderson, T., Sarnthein, M., 2000a. Coherent high- and low-latitude climate variability during the Holocene warm period. Science 288, 2198–2202.

deMenocal, P., Ortiz, J., Guilderson, T., Adkins, J., Sarnthein, M., Baker, L., Yarusinsky, M., 2000b. Abrupt onset and termination of the African humid period. Rapid climate responses to gradual insolation forcing. Quat. Sci. Rev. 19, 347–361.

Domack, E., Leventer, A., Dunbar, R., Taylor, F., Brachfeld, S., Sjunneskog, C., 2001. Chronology of the Palmer Deep site, Antarctic Peninsula: a Holocene palaeoenvironmental reference for the circum-Antarctic. Holocene 11 (1), 1–9.

Garreaud, R.D., 1999. Multiscale analysis of the summertime precipitation over the central Andes. Mon. Weather Rev. 127, 901–921.

Garreaud, R.D., 2000. Intraseasonal variability of moisture and rainfall over the South American Altiplano. Mon. Weather Rev. 128, 3337–3346.

Greenland, D.J., 1971. Interactions between humic and fulvic acids and clays. Soil Sci. 111, 34–41.

Grootes, P.M., Stuiver, M., White, J.W.C., Johnsen, S., Jouzel, J., 1993. Comparison of oxygen isotope records from the GISP2 and GRIP Greenland ice cores. Nature 366, 552–555.

Gu, B., Schmitt, J., Chen, Z., Liang, L., McCarthy, J.F., 1994. Adsorption and desorption of natural organic matter on iron oxide, Mechanisms and models. Environ. Sci. Technol. 28, 38–46.

Gu, B., Schmitt, J., Chen, Z., Liang, L., McCarthy, J.F., 1995. Adsorption and desorption of different organic matter fractions on iron oxide. Geochim. Cosmochim. Acta 59, 219–229.

Guilderson, T.P., Fairbanks, R.G., Rubenstone, J.L., 1994. Tropical temperature variations since 20,000 years ago. Modulating interhemispheric climate change. Science 263, 663–665.

Guilderson, T.P., Fairbanks, R.G., Rubenstone, J.L., 2001. Tropical Atlantic coral oxygen isotopes. Glacial–interglacial sea surface temperatures and climate change. Mar. Geol. 172, 75–89.

Hammarlund, D., Aravena, R., Barnekow, L., Buchardt, B., Possnert, G., 1997. Multi-component carbon isotope evidence of early Holocene environmental change and carbon-flow pathways from a hard-water lake in northern Sweden. J. Paleolimnol. 18, 219–233.

Hatcher, P.G., Breger, I.A., Maciel, G.E., Szeverenyi, N.M., 1985. Geochemistry of humin. In: Aiken, G.R., McKnight, D.M., Wershaw, R.L. (Eds.), Humic Substances in Soil, Sediment, and Water. Geochemistry, Isolation, and Characterization. Wiley, New York, NY, pp. 275–302.

Head, M.J., Zhou, W., Zhou, M., 1989. Evaluation of ^{14}C ages of organic fractions of paleosols from loess–paleosol sequences near Xian, China. Radiocarbon 31 (3), 680–696.

Hedges, J.I., Kiel, R.G., 1999. Organic geochemical perspectives on estuarine processes. Sorption reactions and consequences. Mar. Chem. 65, 55–65.

Jardine, P.M., Weber, N.L., McCarthy, J.F., 1989. Mechanisms of dissolved organic carbon adsorption on soil. J. Soil Sci. Soc. Am. 53, 1378–1385.

Jouzel, J., Waelbroeck, C., Malaize, B., Bender, M., Petit, J.R., Stievenard, M., Barkov, N.I., Barnola, J.M., King, T., Kotlyakov, V.M., Lipenkov, V., Lorius, C., Raynaud, D., Ritz, C., Sowers, T., 1996. Climatic interpretation of the recently extended Vostok ice records. Clim. Dyn. 12, 513–521.

Kiel, R.G., Montluçon, D.B., Prahl, F.G., Hedges, J.I., 1994. Sorptive preservation of labile organic matter in marine sediments. Nature 370, 549–552.

Lenters, J.D., Cook, K.H., 1999. Summertime precipitation variability over South America. Role of the large-scale circulation. Mon. Weather Rev. 127, 409–431.

Lowe, J.J., 1991. Stratigraphic resolution and radiocarbon dating of Devensian lateglacial sediments. Quat. Proc. 1, 19–25.

Lowe, J.J., Walker, M.J.C., 2000. Radiocarbon dating the last glacial–interglacial transition (CA. 14–9 ka BP) in terrestrial and marine records. The need for new quality assurance protocols. Radiocarbon 40, 53–68.

Martin, L., Fournier, M., Mourguiart, P., Sifeddine, A., Turcq, B., Absy, L.M., Flexor, J.M., 1993. Southern oscillation signal in South America paleoclimatic data of the last 7000 years. Quat. Res. 39, 338–346.

Mathewes, R.W., Westgate, J.A., 1980. Bridge River Tephra. Revised distribution and significance for detecting old carbon errors in radiocarbon dates of limnic sediments in southern British Columbia. Can. J. Earth Sci. 17, 1454–1461.

Monnheim, F., 1956. Beiträge zur klimatologie und hydrologie des Titicacabeckens. Heidelb. Geogr. Arb. p. 152.

Mourguiart, P., 1990. Une approche nouvelle du probleme posé par les reconstrutions des paléoniveaux lacustres: utilisation d'une fontion de transfert basée sur les faunes d'ostracodes. Géodynamique 5, 151–166.

Mourguiart, P., Correge, T., Wirrmann, D., Argollo, J., Montenegro, M.E., Pourchet, M., Carbonel, P., 1998. Holocene paleohydrology of Lake Titicaca estimated from an ostracod-based transfer function. Palaeogeogr. Palaeoclimatol. Palaeoecol. 143, 51–72.

Nelson, R.E., Carter, L.D., Robinson, S.W., 1988. Anomalous radiocarbon ages from a Holocene detrital organic lens in Alaska and their implications for radiocarbon dating and paleoenvironmental reconstructions in the Arctic. Quat. Res. 29, 66–71.

Pilcher, J.R., 1991. Radiocarbon dating for the Quaternary scientist. Quat. Proc. 1, 27–33.

Preston, M.R., Riley, J.P., 1982. The interactions of humic compounds with electrolytes and three clay minerals under simulated estuarine conditions. Estuar. Coast. Shelf Sci. 14, 567–576.

Rashid, M.A., 1971. Role of humic acids of marine origin and their different molecular weight fractions in complexing di- and trivalent metals. Soil Sci. 111, 298–306.

Rashid, M.A., King, L.H., 1970. Major oxygen-containing functional groups present in humic and fulvic fractions isolated from contrasting marine environments. Geochim. Cosmochim. Acta 34, 193–201.

Rashid, M.A., Buckley, D.E., Robertson, K.R., 1972. Interactions of a marine humic acid with clay minerals and a natural sediment. Geoderma 8, 11–27.

Roche, M.A., Bourges, J., Cortes, J., Mattos, R., 1992. Climatology and hydrology of the Lake Titicaca basin. In: Dejoux, C., Iltis, A. (Eds.), Lake Titicaca. A Synthesis of Limnological Knowledge. Kluwer Academic Publishing, Dordrecht, The Netherlands, pp. 63–88.

Rodrigo, L.A., Wirrmann, D., 1992. General aspects of present day sedimentation. In: Dejoux, C., Iltis, A. (Eds.), Lake Titicaca. A Synthesis of Limnological Knowledge Kluwer. Academic Publishing, Dordrecht, The Netherlands, pp. 23–28.

Rowe, H.D., Dunbar, R.B., Mucciarone, D.A., Seltzer, G.O., Baker, P.A., Fritz, S.C., 2002. Insolation, moisture balance, and climate change on the South American Altiplano since the last glacial maximum. Clim. Change 52, 175–199.

Sandweiss, D.H., Maasch, K.A., Burger, R.L., Richardson III, J.B., Rollins, H.B., Clement, A., 2001. Variation in Holocene El Niño frequencies: climate records and cultural consequences in ancient Peru. Geology 29, 603–606.

Schnitzer, M., Kodama, H., 1967. Reactions between a podzol fulvic acid and Na-montmorillonite. Proc. Soil Sci. Soc. Am. 31, 632–636.

Schoute, J.F., Mook, M.G., Streurerman, H.J., 1983. Radiocarbon dating of vegetation horizons. In: Mook, W.G., Waterbolk, H.T. (Eds.), Groningen Conference on ^{14}C and Archaeology. Proc. PACT Publ. 8. Université Catholique de Louvain, Louvain-la-Nueve, Belgium, pp. 295–311.

Seltzer, G.O., Baker, P.A., Cross, S., Dunbar, R.B., Fritz, S., 1997. High-resolution seismic reflection profiles from Lake Titicaca, Peru–Bolivia. Evidence for Holocene aridity in the tropical Andes. Geology 26, 167–170.

Shore, J.S., Bartley, D.D., Harkness, D.D., 1995. Problems encountered with the ^{14}C dating of peat. Quat. Sci. Rev. 14, 373–383.

Shotton, F.W., 1972. An example of hard water error in radiocarbon dating of vegetable matter. Nature 240, 460–461.

Steig, E.J., Brook, E.J., White, J.W.C., Sucher, C.M., Bender, M.L., Lehman, S.J., Morse, D.L., Waddington, E.D., Clow, G.D., 1998. Synchronous climate changes in Antarctica and the North Atlantic. Science 282, 92–95.

Stuiver, M., Polach, H.A., 1977. Discussion. Reporting of ^{14}C data. Radiocarbon 19, 355–363.

Stuiver, M., Reimer, P.J., 1993. Extended ^{14}C database and revised CALIB radiocarbon calibration program. Radiocarbon 35, 215–230.

Stuiver, M., Reimer, P.J., Bard, E., Beck, J.W., Burr, G.S., Hughen, K.A., Kromer, B., McCormac, F.G., v. d. Plicht, J., Spurk, M., 1998. INTCAL98 radiocarbon age calibration 24,000–0 cal BP. Radiocarbon 40, 1041–1083.

Tapia, P., Fritz, S.C., Baker, P.A., Seltzer, G.O., manuscript in preparation. A late-Quaternary diatom record of tropical climate history from Lake Titicaca, Bolivia/Peru. Palaeogeogr., Palaeoclimatol., Palaeoecol.

Thimsen, C.A., Kiel, R.G., 1998. Potential interactions between sedimentary dissolved organic matter and mineral surfaces. Mar. Chem. 62, 65–76.

Thompson, L.E., Davis, M.E., Mosley-Thompson, E., Sowers, T.A., Henderson, K.A., Zagorodov, V.S., Lin, P.-N., Mikhalenko, V.N., Campen, R.K., Bolzan, J.F., Cole-Dai, J., Francou, B., 1998. A 25,000-year tropical climate history from Bolivian ice cores. Science 282, 1858–1864.

Van Klinken, G.J., Hedges, R.E.M., 1998. Chemistry strategies for organic ^{14}C samples. Radiocarbon 40 (1), 51–56.

Vuille, M., 1999. Atmospheric circulation over the Bolivian Altiplano during dry and wet periods and extreme phases of the Southern Oscillation. Int. J. Clim. 19, 1579–1600.

Vuille, M., Bradley, R.S., Keimig, F., 2000. Interannual climate variability in the central Andes and their relation to tropical Pacific and Atlantic forcing. J. Geophys. Res. 105, 12.447–12.460.

Wang, X.-C., Lee, C., 1993. Adsorption and desorption of aliphatic amines, amino acids, and acetate by clay minerals and marine sediments. Mar. Chem. 44, 1–23.

Wassenaar, L., Aravena, R., Fritz, P., Barker, J., 1990. Isotopic composition (^{13}C, ^{14}C, ^{2}H) and geochemistry of aquatic humic substances from groundwater. Org. Geochem. 15 (4), 383–396.

Wirrmann, J.P., 1992. Morphology and bathymetry. In: Dejoux, C., Iltis, A. (Eds.), Lake Titicaca. A Synthesis of Limnological Knowledge. Kluwer Academic Publishing, Dordrecht, The Netherlands, pp. 16–23.

Wirrmann, D., Fernando De Oliveira Almeida, L., 1987. Low Holocene level (7700 to 3650 years ago) of Lake Titicaca (Bolivia). Palaeogeogr. Palaeoclimatol. Palaeoecol. 59, 315–323.

Wirrmann, D., Mourguiart, P., 1995. Late Quaternary spatio–temporal limnological variations in the Altiplano of Bolivia and Peru. Quat. Res. 43, 344–354.

Wirrmann, D., Mourguiart, P., Fernando de Oliveira Almeida, L., 1990. Holocene sedimentology and ostracods distribution in Lake Titicaca-paleohydrological interpretations. In: Rabassa, J. (Ed.), Quaternary of South America and Antarctic Peninsula, vol. 6. A.A. Balkema, Rotterdam, pp. 89–129.

Wirrmann, J.P., Ybert, J.P., Mourguiart, P., 1992. A 20,000 years paleohydrological record from Lake Titicaca. In: Dejoux, C., Iltis, A. (Eds.), Lake Titicaca. A Synthesis of Limnological Knowledge. Kluwer Academic Publishing, Dordrecht, The Netherlands, pp. 40–48.

Zhou, J., Lau, K.-M., 1998. Does a monsoon climate exist over South America? J. Clim. 11, 1020–1040.